

1 **Supporting Information**

2

3 **Primary and secondary emissions from a modern fleet of city buses**

4 Liyuan Zhou^{1,2#}, Qianyun Liu^{2,a#}, Christian M. Salvador^{3,b}, Michael Le Breton^{3,c}, Mattias Hallquist³, Jian
5 Zhen Yu⁴ and Chak K. Chan^{1,2*}, Åsa M. Hallquist^{5*}

6

7 ¹ Division of Physical Sciences and Engineering, King Abdullah University of Science and Technology, Thuwal, Saudi Arabia

8 ² School of Energy and Environment, City University of Hong Kong, Hong Kong SAR, China

9 ³ Department of Chemistry and Molecular Biology, University of Gothenburg, Gothenburg, Sweden

10 ⁴ Division of Environment and Sustainability, Hong Kong University of Science and Technology, Hong Kong, China

11 ⁵ IVL Swedish Environmental Research Institute, Gothenburg, Sweden

12 ^anow at: RELX Science Center, Shenzhen RELX Tech. Co., Ltd., Shenzhen, China

13 ^bnow at: Environmental Sciences Division, Oak Ridge National Laboratory, Oak Ridge, TN 37830, USA

14 ^cnow at: FEV Sverige AB, Gothenburg, Sweden

15

16

17 [#]The authors contribute equally.

18 *Correspondence to:* Åsa M Hallquist (asa.hallquist@ivl.se); Chak K. Chan (chak.chan@kaust.edu.sa)

19

20 Text S1. Mass-to-charge ratio (m/z) calibration.

21 In this study, six isolated ion peaks (O_2^- , CNO^- , $C_3H_5O_3^-$, $C_2F_3O_3^-$, $C_5F_9O_2^-$, $C_{10}HF_9O_4^-$) were identified as suitable for m/z
22 calibration over the entire studied m/z range. Accuracies are reported as parts-per-million of the m/z value (ppm), calculated
23 as:

$$24 \text{ Accuracy [ppm]} = (m/z_{\text{comp}} - m/z_{\text{cal}}) / (m/z_{\text{cal}}) \times 10^6, \quad (1)$$

25 where m/z_{comp} is the peak position, m/z_{cal} is the calibration value. The average accuracy achieved for all six m/z calibrants was
26 within 3 ppm (Table S1), determined from a weighted average of all m/z calibration accuracies and their standard deviations.
27 The accuracy for ions not used in the m/z calibration is also evaluated. Several overlapping peaks are recorded at most integer
28 m/z, and multi-peak fitting is performed to determine individual signal intensities (Figure S3). This procedure may introduce
29 additional uncertainty in the determined peak positions beyond the m/z accuracy of isolated peaks. To estimate the accuracy
30 for the measured ions, multi-peak fits of peaks with known individual peak positions were performed. Table S2 shows the
31 average biases and m/z accuracies for five (Cl^- , NO_2^- , NO_3^- , $C_3H_5O_3^-$, $C_3H_{15}O_2^-$) ions, determined from a time series of several
32 hours of individual spectra. The table lists values for both isolated peaks and those in multiple-peak groups. The average
33 accuracies estimated for the isolated peaks are similar to those for the m/z calibration peaks, but larger for the multiple peak
34 cases, reflecting the additional uncertainties due to the proximity of other peaks.

35

36 Text S2. OH exposure in Go:PAM.

37 The OH_{exp} in Go:PAM was calculated using the model described by Watne et al. (2018). Briefly, a chemical model containing
38 a comprehensive description of ozone photolysis and HO_x chemistry and a skeleton description of NO_x , CO, HC and SO_x
39 chemistry was used to mimic the gas-phase chemistry in Go:PAM (Table S3). The minimum OH exposure was derived for
40 each bus passage plume using the maximum NO_x , HC and CO concentrations in Go:PAM and the corresponding water and
41 ozone concentrations. The assumed speciation of HC was aldehydes (26%), alkanes (33%), alkenes (14%) and aromatic
42 compounds (27%). The oxidation capacity of Go:PAM was offline calibrated by SO_2 as described by Lambe et al. (2011),
43 where the photon flux at 254 nm, $P_{\text{FLUX}254} = 1.57 \times 10^{16} \text{ cm}^{-2} \text{ s}^{-1}$, and first order loss rates of OH were derived by matching the
44 measured and modeled SO_2 and O_3 decreases.

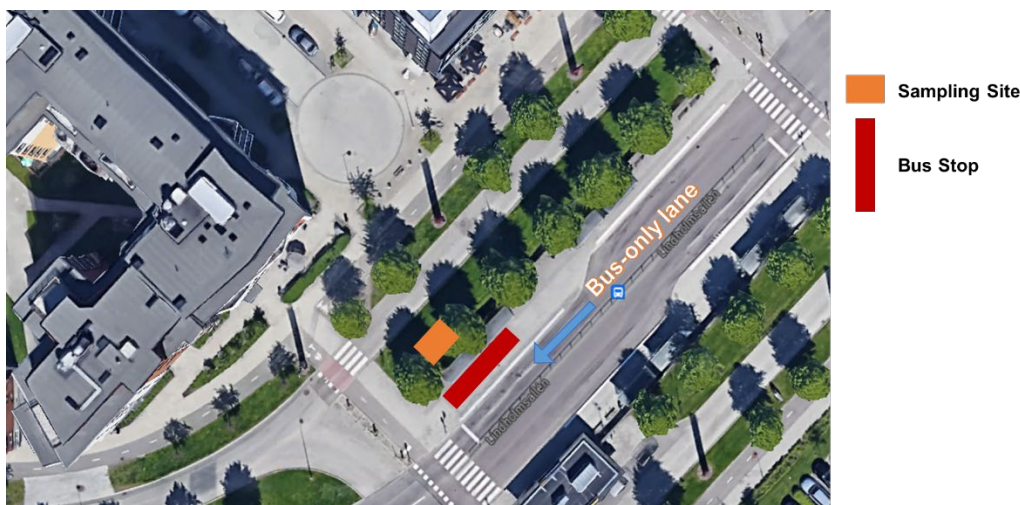
45 Recently, a concern of non-OH chemistry in the OFR has been raised. (Peng et al., 2016) In this study, we estimated the ratios
46 of exposures of non-OH species to OH exposure for O_3 , $O(^1D)$ and $O(^3P)$. The relative importance of non-OH chemistry was
47 evaluated according to Peng et al. (Peng et al., 2016), by taking toluene as a surrogate as it is a common SOA precursor found
48 in vehicle emissions (Gentner et al., 2017; Liu et al., 2019). The undesired VOC destructions by O_3 , $O(^1D)$ and $O(^3P)$ were
49 negligible (close to 0 %). The direct photolysis of aromatics in Go:PAM has been evaluated by Watne et al. (2018) under
50 similar experimental conditions (photon flux, residence time). No reductions of toluene and trimethyl-benzene were observed
51 with UV light on.

52

53 Text S3. Classification of acetate-CIMS measured species.

54 The identities of the organic compounds are assigned based on knowledge of the sensitivities of the ionization scheme and the
55 expected compounds emitted from the buses. These compounds were classified into nine families on the basis of their
56 molecular characteristics, according to Liu et al. (2017). Briefly, the functional group composition of ions containing C, H or
57 O atoms was estimated from its elemental composition using the number of oxygen atoms (n_o) and double bond equivalency
58 (DBE, calculated as $1+n_c-1/2n_H$), assuming (1) each ion has at least one carboxylic acid group, (2) the excess oxygen ($n_o - 2$)
59 is contained in hydroxy or keto groups, (3) the excess DBE (DBE - 1) is due to keto groups (priority) or alkene groups, and
60 (4) a phenyl group exists if $DBE \geq 5$. The ions are categorized into acid classes using the following prioritized criteria: (1) if
61 $DBE \geq 5$, the ion is categorized as an aromatic acid, otherwise (2) if $n_o = 2$, the ion is assigned as a monoacid (either saturated
62 (DBE=1) or unsaturated (DBE>1)), (3) if $n_o > 2$, and $n_o > 2 \times DBE$, the ion is counted as a hydroxy acid, (4) in the case of n_o
63 > 2 and $n_o \leq 2 \times DBE$ (DBE ≥ 2), the ions is defined as a carbonyl acid if n_o is an odd number, otherwise the ion is referred to
64 as a diacid or hydroxycarbonyl acid. For ions containing N or S atoms, (1) if the $n_N > 0$, and $n_S = 0$, ions is assigned as a nitrogen
65 (N)-containing compounds (no S), (2) if the $n_S > 0$, and $n_N = 0$, ions is assigned as a sulfur (S)-containing compounds (no N),
66 (3) if the $n_N > 0$, and $n_S > 0$, ions is assigned as a N and S-containing compounds. Table S4 lists the classification for the ions
67 identified in this study.

68

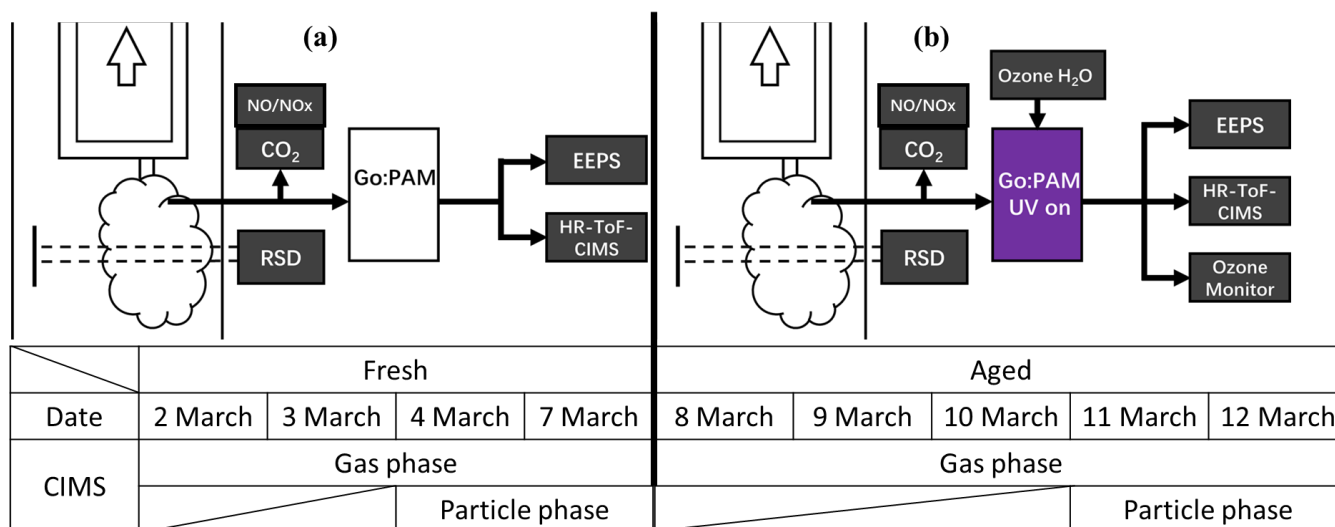


70

71 Figure S1. Satellite image of the roadside sampling site at Lindholmen, Gothenburg, Sweden. Map data: © Google, DigitalGlobe.

72

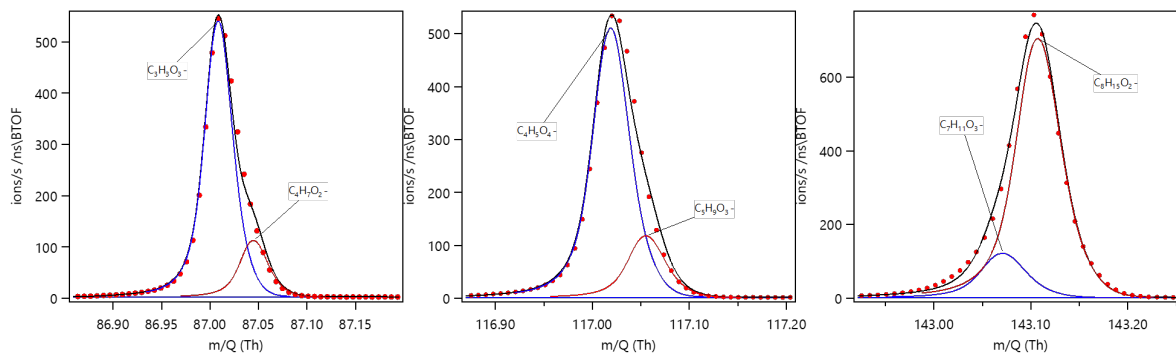
73



74

75 Figure S2. Schematic of the roadside measurement. (a) fresh emission measurements, (b) aged measurements: photo-oxidation
76 of bus plumes. RSD (Remote Sensing Device), CO₂ analyzer, NO/NO_x analyser, EEPS (Engine Exhaust Particle Sizer), and
77 HR-ToF-CIMS (high-resolution time-of-flight chemical-ionization mass spectrometer).

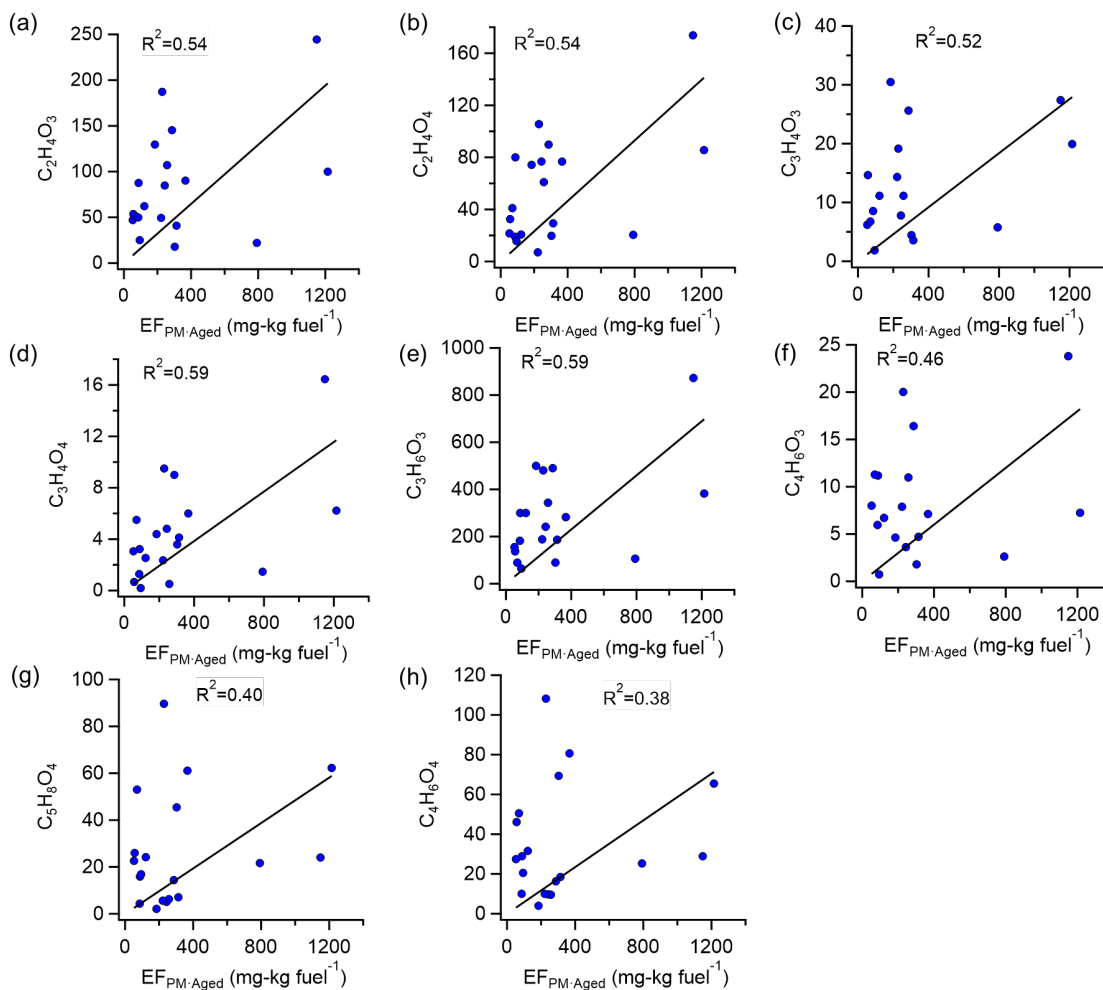
78



79

80 Figure S3. Example peak fits of major ions.

81



82

83 Figure S4. Correlations between ion counts of most abundant gas-phase organic acids and $EF_{PM:aged}$ (a-h) from 19 buses after
 84 oxidation in the Go:PAM.

85

86 Table S1. Isolated ion peaks for m/z calibration.

Exact, m/z	Assigned formula	Accuracy $\pm 1\sigma$ (ppm)
31.990378	O ₂ ⁻	0.2 \pm 0.1
41.998537	CNO ⁻	2.6 \pm 1.1
89.024418	C ₃ H ₅ O ₃ ⁻	2.9 \pm 2
112.985587	C ₂ F ₃ O ₃ ⁻	3.2 \pm 2.7
262.976007	C ₅ F ₉ O ₂ ⁻	3.1 \pm 1

87

88

89 Table S2. The average biases and m/z accuracies for five ions (determined from a time series of several hours of individual
90 spectra).

Exact, m/z	Assigned formula	Accuracy ± 1 (ppm)	Comments
34.969401	Cl ⁻	3.7 \pm 3.2	Isolate peak
89.024418	C ₃ H ₅ O ₃ ⁻	1.5 \pm 1.2	Isolate peak
61.988366	NO ₃ ⁻	1.2 \pm 1	Isolate peak
45.993452	NO ₂ ⁻	2.8 \pm 1.2	Isolate peak
143.107753	C ₈ H ₁₅ O ₂ ⁻	3.7 \pm 5	Multi-peak

91

92

93

94

95 Table S3. Reactions and rate coefficients for model calculations of OH exposure. The data were taken from the literature as
96 described in Watne et al. * 74% of measured HC, **26% of measured HC.

No.	Reaction	k (cm ³ molecule ⁻¹ s ⁻¹)
1	O ₃ +hν → O ₂ +O(¹ D)	0.18
2	O(¹ D)+H ₂ O → OH+OH	1.99 $\times 10^{-10}$
3	O(¹ D)+O ₂ → O(³ p)+O ₂	3.97 $\times 10^{-11}$
4	O(¹ D)+O ₃ → O ₂ +O(³ p)+ O(³ p)	1.2 $\times 10^{-10}$
5	O(¹ D)+O ₃ → O ₂ + O ₂	1.2 $\times 10^{-10}$
6	O(¹ D)+N ₂ → O(³ p)+N ₂	3.11 $\times 10^{-11}$
7	O(³ p)+O ₂ +M → O ₃ +M	6.1 $\times 10^{-34}$
8	O(³ p)+O ₃ → O ₂ +O ₂	7.96 $\times 10^{-15}$
9	O(³ p)+OH → H+O ₂	3.29 $\times 10^{-11}$
10	H+O ₂ → HO ₂	9.57 $\times 10^{-13}$
11	H+HO ₂ → OH+OH	7.2 $\times 10^{-11}$
12	H+HO ₂ → O(³ p)+H ₂ O	1.6 $\times 10^{-12}$
13	H+HO ₂ → H ₂ +O ₂	6.9 $\times 10^{-12}$
14	OH+OH → H ₂ O+O(³ p)	1.8 $\times 10^{-12}$

15	$\text{OH}+\text{OH} \rightarrow \text{H}_2\text{O}_2$	6.29×10^{-12}
16	$\text{OH}+\text{O}_3 \rightarrow \text{HO}_2+\text{O}_2$	7.25×10^{-14}
17*	$\text{HO}_2+\text{HO}_2 \rightarrow \text{H}_2\text{O}_2+\text{O}_2$	3.28×10^{-12}
18**	$\text{HC}+\text{OH} \rightarrow 0.7\text{RO}_2+0.3\text{HO}_2$	1.0×10^{-11}
19	$\text{HCHO}+\text{OH} \rightarrow \text{H}_2\text{O}+\text{CO}+\text{HO}_2$	9.2×10^{-12}
20	$\text{SO}_2+\text{OH} \rightarrow \text{OHSO}_2$	9.59×10^{-13}
21	$\text{OHSO}_2+\text{O}_2 \rightarrow \text{SO}_3+\text{HO}_2$	4.3×10^{-13}
22	$\text{NO}+\text{O}(^3\text{p}) \rightarrow \text{NO}_2$	1.66×10^{-12}
23	$\text{NO}_2+h\nu \rightarrow \text{NO}+\text{O}(^3\text{p})$	1.64×10^{-4}
24	$\text{NO}_2+\text{OH} \rightarrow \text{HNO}_3$	1.06×10^{-11}
25	$\text{NO}_2+\text{OH} \rightarrow \text{HOONO}$	1.79×10^{-12}
26	$\text{HO}_2+\text{NO} \rightarrow \text{NO}_2+\text{OH}$	8.16×10^{-12}
27	$\text{RO}_2+\text{NO} \rightarrow \text{RO}+\text{NO}_2$	9×10^{-12}
28	$\text{O}(^1\text{D})+\text{N}_2+\text{M} \rightarrow \text{N}_2\text{O}+\text{M}$	2.82×10^{-36}
29	$\text{N}_2\text{O}+\text{O}(^1\text{D}) \rightarrow \text{N}_2+\text{O}_2$	5.09×10^{-11}
30	$\text{N}_2\text{O}+\text{O}(^1\text{D}) \rightarrow \text{NO}+\text{NO}$	7.64×10^{-11}
31	$\text{O}(^3\text{p})+\text{HO}_2 \rightarrow \text{OH}+\text{O}_2$	5.87×10^{-11}
32	$\text{O}(^3\text{p})+\text{H}_2\text{O}_2 \rightarrow \text{OH}+\text{HO}_2$	1.7×10^{-15}
33	$\text{H}+\text{O}_3 \rightarrow \text{OH}+\text{O}_2$	2.89×10^{-11}
34	$\text{HO}_2+\text{O}_3 \rightarrow \text{OH}+\text{O}_2+\text{O}_2$	1.93×10^{-15}
35	$\text{HO}_2+\text{OH} \rightarrow \text{H}_2\text{O}+\text{O}_2$	1.11×10^{-10}
36	$\text{H}_2\text{O}_2+h\nu \rightarrow \text{OH}+\text{OH}$	1.05×10^{-3}
37	$\text{HO}_2+h\nu \rightarrow \text{OH}+\text{O}(^1\text{D})$	4.07×10^{-3}
38	$\text{OH}+\text{H}_2\text{O}_2 \rightarrow \text{HO}_2+\text{H}_2\text{O}$	1.8×10^{-12}
39	$\text{NO}+\text{O}_3 \rightarrow \text{NO}_2+\text{O}_2$	1.95×10^{-14}
40	$\text{O}(^1\text{D})+\text{H}_2 \rightarrow \text{OH}+\text{H}$	1.2×10^{-10}
41	$\text{OH}+\text{H}_2 \rightarrow \text{H}_2\text{O}+\text{H}$	6.67×10^{-15}
42	$\text{NO}_2+\text{O}(^3\text{p}) \rightarrow \text{NO}+\text{O}_2$	1.03×10^{-11}
43	$\text{NO}_2+\text{O}(^3\text{p}) \rightarrow \text{NO}_3$	1.61×10^{-12}
44	$\text{H}+\text{NO}_2 \rightarrow \text{NO}+\text{OH}$	1.28×10^{-10}
45	$\text{NO}+\text{NO}_3 \rightarrow \text{NO}_2+\text{NO}_2$	2.65×10^{-11}
46	$\text{NO}_2+\text{O}_3 \rightarrow \text{NO}_3+\text{O}_2$	3.2×10^{-17}
47	$\text{CO}+\text{OH} \rightarrow \text{CO}_2+\text{H}$	2.4×10^{-13}
48	OH deposition/loss	35
49	$\text{CH}_3\text{O} \rightarrow \text{HCHO}+\text{HO}_2$	9.92×10^3
50	$\text{CH}_3\text{OH}+\text{OH} \rightarrow \text{HO}_2+\text{HCHO}$	8.95×10^{-13}
51	$\text{OH}+\text{CH}_3\text{OOH} \rightarrow \text{HCHO}+\text{OH}$	4.01×10^{-12}
52	$\text{OH}+\text{CH}_3\text{OOH} \rightarrow \text{CH}_3\text{O}_2$	6.02×10^{-12}
53	$\text{CH}_3\text{O}_2+\text{CH}_3\text{O}_2 \rightarrow \text{CH}_3\text{OH}+\text{HCHO}$	4.43×10^{-13}
54	$\text{CH}_3\text{O}_2+\text{CH}_3\text{O}_2 \rightarrow \text{CH}_3\text{O}+\text{CH}_3\text{O}$	2.58×10^{-13}
55	$\text{CH}_3\text{O}_2+\text{NO}_2 \rightarrow \text{CH}_3\text{O}_2\text{NO}_2$	5.88×10^{-12}
56	$\text{CH}_3\text{O}_2\text{NO}_2 \rightarrow \text{CH}_3\text{O}_2+\text{NO}_2$	1.50
57	$\text{OH}+\text{CH}_4 \rightarrow \text{CH}_3\text{O}_2$	6.37×10^{-15}
58	$\text{CH}_3\text{O}_2+\text{HO}_2 \rightarrow \text{CH}_3\text{OOH}$	4.74×10^{-12}
59	$\text{CH}_3\text{O}_2+\text{HO}_2 \rightarrow \text{HCHO}$	4.67×10^{-13}
60	$\text{CH}_3\text{O}_2+\text{NO} \rightarrow \text{CH}_3\text{O}+\text{NO}_2$	7.69×10^{-12}

97

98

99

100

101

102

103 Table S4. Classification of acetate-CIMS measured species.

Elemental composition	Formula	Assigned category
No N or S	DBE=1-3, $n_o=2$	monoacid
	DBE=2-3, $n_o=4$	diacid/hydroxycarbonyl acid
	DBE = 1, $n_o = 3-5$ or DBE = 2, $n_o>4$	hydroxy acid
	DBE = 2, $n_o = 3$ or DBE = 3, $n_o\leq 6$	carbonyl acid
	DBE = 5 or 6, $n_o = 2-5$	aromatic acid
With N or S	$n_N> 0$, and $n_S=0$	nitrogen (N)-containing compounds (no S)
	$n_S> 0$, and $n_N=0$	sulfur (S)-containing compounds (no N)
	$n_N> 0$, and $n_S>0$	N and S-containing compounds

104

105

106

107

108 **Reference**

- 109 Gentner, D. R., Jathar, S. H., Gordon, T. D., Bahreini, R., Day, D. A., El Haddad, I., Hayes, P. L., Pieber, S. M., Platt, S. M., de Gouw, J.,
110 Goldstein, A. H., Harley, R. A., Jimenez, J. L., Prevot, A. S., and Robinson, A. L.: Review of Urban Secondary Organic Aerosol Formation
111 from Gasoline and Diesel Motor Vehicle Emissions, *Environ Sci Technol*, 51, 1074-1093, <https://doi.org/10.1021/acs.est.6b04509>, 2017.
112 Lambe, A. T., Ahern, A. T., Williams, L. R., Slowik, J. G., Wong, J. P. S., Abbatt, J. P. D., Brune, W. H., Ng, N. L., Wright, J. P., Croasdale,
113 D. R., Worsnop, D. R., Davidovits, P., and Onasch, T. B.: Characterization of aerosol photooxidation flow reactors: heterogeneous oxidation,
114 secondary organic aerosol formation and cloud condensation nuclei activity measurements, *Atmos. Meas. Tech.*, 4, 445-461, 10.5194/amt-
115 4-445-2011, 2011.
116 Liu, S., Thompson, S. L., Stark, H., Ziemann, P. J., and Jimenez, J. L.: Gas-phase carboxylic acids in a university classroom: Abundance,
117 variability, and sources, *Environmental Science & Technology*, 51, 5454-5463, 2017.
118 Liu, T., Zhou, L., Liu, Q., Lee, B. P., Yao, D., Lu, H., Lyu, X., Guo, H., and Chan, C. K.: Secondary organic aerosol formation from urban
119 roadside air in Hong Kong, *Environmental science & technology*, 53, 3001-3009, <https://doi.org/10.1021/acs.est.8b06587>, 2019.
120 Peng, Z., Day, D. A., Ortega, A. M., Palm, B. B., Hu, W., Stark, H., Li, R., Tsigaridis, K., Brune, W. H., and Jimenez, J. L.: Non-OH
121 chemistry in oxidation flow reactors for the study of atmospheric chemistry systematically examined by modeling, 2016.
122 Watne, A. K., Psichoudaki, M., Ljungstrom, E., Le Breton, M., Hallquist, M., Jerksjo, M., Fallgren, H., Jutterstrom, S., and Hallquist, A.
123 M.: Fresh and Oxidized Emissions from In-Use Transit Buses Running on Diesel, Biodiesel, and CNG, *Environ Sci Technol*, 52, 7720-7728,
124 <https://doi.org/10.1021/acs.est.8b01394>, 2018.

125